



Secrecy Performance Enhancement Using Path Selection over Cluster-Based Cognitive Radio Networks

Pham Minh Nam¹, Phan Van Ca¹, Tran Trung Duy^{2(✉)}, and Khoa N. Le³

¹ University of Technology and Education, Ho Chi Minh City 700000, Vietnam
1727002@student.hcmute.edu.vn, capv@hcmute.edu.vn

² Posts and Telecommunications Institute of Technology, Ho Chi Minh City, Vietnam
trantrungduy@ptithcm.edu.vn

³ Western Sydney University, Penrith South, NSW, Australia
lenkhoa@gmail.com

Abstract. In this paper, we propose three path selection methods for cluster-based cognitive radio (CR) networks for secrecy enhancement by formulating the probability of non-zero secrecy capacity (PNSC). In the proposed work, it is assumed that uniform transmit power for the secondary transmitters and jammers must be adjusted to guarantee quality of service (QoS) of the primary network, follows a simple and efficient power allocation strategy. To improve the channel capacity, the best receiver is selected at each cluster to relay the source data to the next hop. Additionally, a jammer is randomly chosen at each cluster to generate noises on an eavesdropper, and to reduce the quality of the eavesdropping links. Three methods are studied in this paper. First, we propose the BEST path selection method (BEST) to maximize the end-to-end instantaneous secrecy capacity. Second, the path obtaining the MAXimum Value for the average end-to-end PNSC (MAXV) is selected for data transmission. Third, we also propose a RAND method in which a RANDOM path is employed. For performance evaluation and comparison, we derive exact closed-form expressions for the end-to-end PNSC of the BEST, MAXV and RAND methods over Rayleigh fading channel. Monte Carlo simulations are then performed to verify the derived theoretical results.

Keywords: Physical-layer security · Cognitive radio · Cluster networks · Path selection · Secrecy capacity

1 Introduction

Physical-layer security (PLS) [1,2] has recently emerged as an efficient method to provide security for wireless sensor networks (WSNs) and Internet of Things (IoT) networks. Under PLS context, secure communication can be obtained when

channel capacity of a data link is higher than that of an eavesdropping link. Therefore, diversity-based transmit/receive methods [3–5] and cooperative relaying transmission [6–8] have been widely used to enhance secrecy performance, in terms of average secrecy capacity (ASC), secrecy outage probability (SOP), and probability of non-zero secrecy capacity (PNSC). Additionally, the methods reported in [3–8] can be combined with cooperative jamming techniques reported in [9, 10], i.e., jammers can practically collude with authorized receivers so that generated artificial noise can only interfere on the eavesdropper nodes.

Until now, there have been only several published works for performance evaluation of multi-hop transmission in PLS [8, 11–14]. In [11], authors proposed a cluster-based secure communication with relay selection methods at each hop. In addition, the eavesdropper in [11] can use maximal ratio combining (MRC) to decode the data received over multiple hops. In [12], authors developed a system model by combining a randomize-and-forward (RF) method and cooperative jamming techniques. Particularly, the transmitters randomly generate codebooks when forwarding the source data, while the selected receivers and jammers collaborate to remove interferences in the received signals. In [13, 14], full-duplex relaying methods for enhancing security over multi-hop relaying systems were proposed and evaluated. Being different with [11–14], authors of [8] considered a multi-hop amplify-and-forward (AF) relaying model in PLS, employing compress sensing.

Recently, PLS in cognitive radio (CR) has gained much attention from researchers. The authors of [15, 16] proposed cooperative cognitive protocols using cooperative jamming to enhance secrecy performance for secondary networks. In [17, 18], radio frequency energy harvesting (RF-EH) based secure communication protocols employing overlay and underlay spectrum sharing approaches were investigated. Authors in [19] focused on designing a routing protocol for cooperative jamming multi-hop multi-antenna secondary networks in the presence of random eavesdroppers. In [20], a cooperative routing scheme was proposed to enhance secrecy performance for multi-hop relaying secondary networks. In [21], authors considered transmit antenna selection (TAS)/selection combining (SC) and harvest-to-transmit based secure multi-hop transmission over underlay CR environments in the presence of multi-antenna eavesdroppers, and hardware imperfection.

To the best of our knowledge, PLS in cluster-based multi-hop multi-path over underlay CR networks has not yet been studied. This has motivated us to propose and evaluate secrecy performance of CR networks. This paper thus focuses on end-to-end PNSC performance of secondary networks, where a secondary source communicates with a secondary destination using a multi-hop multi-path relaying approach. For the underlay spectrum sharing, the secondary transmitters including source and relays must adjust their transmit power to satisfy QoS of the primary network. Under this power constraint, we propose the best receiver selection at each cluster to improve data transmission reliability. On the other hand, to lessen the severity of eavesdropping channels, a jammer at each cluster is randomly selected to realize the effectiveness of the coopera-

tive jamming process. The main contributions of this paper are summarized as follows:

- We propose a simple power allocation strategy for the secondary transmitters and jammers to satisfy the required primary QoS.
- We propose three efficient path selection methods, BEST, MAXV and RAND. For the BEST method, the path with the highest end-to-end instantaneous secrecy capacity is chosen for data transmission. For the MAXV method, the system selects the path obtaining maximum value of the average end-to-end PNSC. For the RAND method, a random path is used to transmit source data to the destination.
- We derive exact closed-form expressions for the end-to-end PNSC of the BEST, MAXV and RAND methods over Rayleigh fading channels, which are then verified by Monte Carlo simulation.

The remainder of this paper is organized as follows. The system model of the considered methods is described in Sect. 2. In Sect. 3, expressions for the end-to-end PNSC of the BEST, MAXV and RAND methods are derived. Simulation results are shown in Sect. 4 to verify the derived theoretical results. Finally, Sect. 5 concludes the main findings and outlines possible future work.

2 System Model

Figure 1 presents the system model for the proposed underlay CR network, where the primary network shares licensed bands to the secondary network. For the primary network, the primary transmitter (PT) sends its data to the primary receiver (PR). In the secondary network, the source S attempts to transmit its data to the destination D using the multi-hop relaying approach, in the presence of the eavesdropper E, who illegally listens to the source data. Assuming that there are M available disjoint paths that are established at the network layer, and the source would select one path for the data transmission. On the m -th path, there are N_m clusters between S and D, denoted by $CL_{m,1}, CL_{m,2}, \dots, CL_{m,N_m}$, where $m = 1, 2, \dots, M$ and $N_m \geq 1$. We also denote $CL_{m,0}$ and CL_{m,N_m+1} as the clusters including the source and the destination, respectively. In addition, let us denote $L_{m,u}$ as the number of nodes belonging to the cluster $CL_{m,u}$, and $\{R_{m,u,1}, R_{m,u,2}, \dots, R_{m,u,L_{m,u}}\}$ as the set of these nodes, where $u = 1, 2, \dots, N_m$. Considering the cluster CL_{m,N_m+1} , except the destination, the remaining cluster nodes are named as $R_{m,N_m+1,2}, \dots, R_{m,N_m+1,L_{m,N_m+1}}$, where $L_{m,N_m+1} = L_D (\forall m)$. Figure 1 presents the system model for the proposed underlay CR network, where the primary network shares licensed bands to the secondary network. For the primary network, the primary transmitter (PT) sends its data to the primary receiver (PR). In the secondary network, the source S attempts to transmit its data to the destination D using the multi-hop relaying approach, in the presence of the eavesdropper E, who illegally listens to the source data. Assuming that there are M available disjoint paths that are

established at the network layer, and the source would select one path for the data transmission. On the m -th path, there are N_m clusters between S and D, denoted by $CL_{m,1}, CL_{m,2}, \dots, CL_{m,N_m}$, where $m = 1, 2, \dots, M$ and $N_m \geq 1$. We also denote $CL_{m,0}$ and CL_{m,N_m+1} as the clusters including the source and the destination, respectively. In addition, let us denote $L_{m,u}$ as the number of nodes belonging to the cluster $CL_{m,u}$, and $\{R_{m,u,1}, R_{m,u,2}, \dots, R_{m,u,L_{m,u}}\}$ as the set of these nodes, where $u = 1, 2, \dots, N_m$. Considering the cluster CL_{m,N_m+1} , except the destination, the remaining cluster nodes are named as $R_{m,N_m+1,2}, \dots, R_{m,N_m+1,L_{m,N_m+1}}$, where $L_{m,N_m+1} = L_D (\forall m)$.

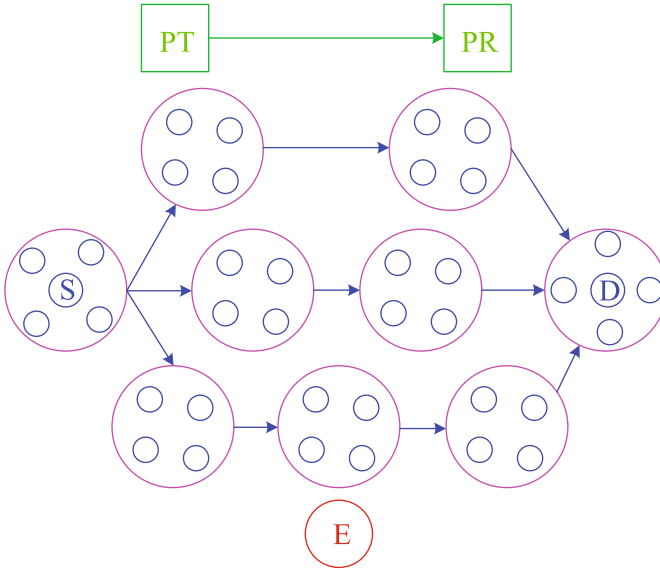


Fig. 1. System model of the proposed methods.

It is assumed that (i) all of the nodes are equipped with single antennas, and operate on the half-duplex mode; (ii) all the channels are block slow Rayleigh fading, which remains coherently constant over the length of a code word. Hence, the channel gain $\gamma_{X,Y}$ of the $X \rightarrow Y$ link is an exponential random variable (RV), where $(X, Y) \in \{PT, PR, R_{m,u,v}, E\}$, $m = 1, 2, \dots, M$, $u = 0, 1, \dots, N_m + 1$, $v = 1, 2, \dots, L_{m,u}$, and $R_{m,0,v} \equiv S$, $R_{m,N_m+1,1} \equiv D (\forall m, v)$. Then, the cumulative distribution function (CDF) and probability density function (PDF) of $\gamma_{X,Y}$ can be expressed, respectively as

$$F_{\gamma_{X,Y}}(z) = 1 - \exp(-\lambda_{X,Y}z), \quad f_{\gamma_{X,Y}}(z) = \lambda_{X,Y} \exp(-\lambda_{X,Y}z), \quad (1)$$

where $\lambda_{X,Y} = d_{X,Y}^{-\beta}$ [22], $d_{X,Y}$ is the link distance between X and Y, and β is the path-loss exponent. Since the nodes in the cluster $CL_{m,u}$ are closely spaced, we

can assume the distances $d_{X,R_{m,u,v}}$ are statistically unchanged, i.e., $d_{X,R_{m,u,v}} = d_{X,R_{m,u,t}} (\forall v, t)$.

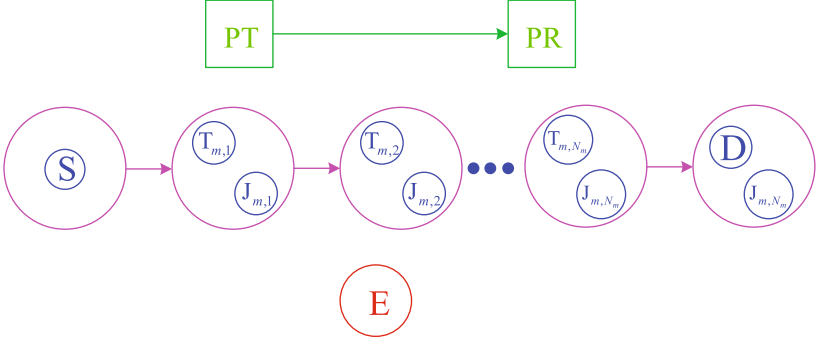


Fig. 2. Data transmission on the m -th path.

Assume that the m -th path is selected (see Fig. 2). Because of the half-duplex constraint, the transmit data stream is split into $N_m + 1$ orthogonal time slots. At the first time slot, the source sends the data to the best node belonging to the cluster $CL_{m,1}$, which is chosen to maximize the channel gain of the first hop as [11]:

$$T_{m,1} : \arg \max_{v=1,2,\dots,L_{m,1}} (\gamma_{S,R_{m,1,v}}), \quad (2)$$

where $T_{m,1}$ denotes the selected node.

Moreover, during the $S \rightarrow T_{m,1}$ transmission, one of the remaining nodes of the cluster $CL_{m,1}$, named $J_{m,1}$, is randomly chosen to generate jamming noise on the eavesdropper E . It is worth noting that $T_{m,1}$ can remove the interference from $J_{m,1}$ via exchanging secure messages with $T_{m,1}$ [12]. Then, after decoding the source data, $T_{m,1}$ re-encodes and forwards it to the next cluster in the second time slot.

Generally, the best receiver at the u -th time slot, named $T_{m,u}$, is selected by

$$T_{m,u} : \arg \max_{v=1,2,\dots,L_{m,u}} (\gamma_{T_{m,u-1},R_{m,u,v}}), \quad (3)$$

where $u = 1, 2, \dots, N_m$, and $T_{m,0} \equiv S$.

Let us consider the last time slot, the transmitter T_{m,N_m} transmits the source data to the destination D , while the jammer J_{m,N_m+1} , a member of the cluster CL_{m,N_m+1} , is employed to realize the cooperative jamming operation. Because the eavesdropper can overhear multiple hops, the transmitters $T_{m,u}$ employ the randomize-and-forward method [12] so that it cannot combine the received signals using MRC.

Considering the data transmission between PT and PR in the u -th time slot of the m -th path, because of the co-channel interference caused by $T_{m,u-1}$ and

$J_{m,u}$, the instantaneous signal-to-interference-plus-noise ratio (SINR) obtained at PR can be formulated by

$$\psi_{\text{PT,PR}}^{(m,u)} = \frac{P_{\text{PT}}\gamma_{\text{PT,PR}}}{P_{\text{T}_{m,u-1}}\gamma_{\text{T}_{m,u-1},\text{PR}} + P_{\text{J}_{m,u}}\gamma_{\text{J}_{m,u},\text{PR}} + \sigma^2}, \quad (4)$$

where P_X is the transmit power of X ($X \in \{\text{PT}, \text{T}_{m,u-1}, \text{J}_{m,u}\}$), and σ^2 is a variance of Additive White Gaussian Noise (AWGN). For brevity, we set $\sigma^2 = 1$ at all of the receivers.

Next, since $\text{T}_{m,u}$ can perfectly remove the interference generated by $\text{J}_{m,u}$, the instantaneous SINR of the $\text{T}_{m,u-1} \rightarrow \text{T}_{m,u}$ link is obtained as

$$\psi_{\text{T}_{m,u-1},\text{T}_{m,u}} = \frac{P_{\text{T}_{m,u-1}}\gamma_{\text{T}_{m,u-1},\text{T}_{m,u}}}{P_{\text{PT}}\gamma_{\text{PT},\text{T}_{m,u}} + 1}. \quad (5)$$

For the $\text{T}_{m,u-1} \rightarrow \text{E}$ link, the instantaneous SINR is written by

$$\psi_{\text{T}_{m,u-1},\text{E}} = \frac{P_{\text{T}_{m,u-1}}\gamma_{\text{T}_{m,u-1},\text{E}}}{P_{\text{PT}}\gamma_{\text{PT},\text{E}} + P_{\text{J}_{m,u}}\gamma_{\text{J}_{m,u},\text{E}} + 1}. \quad (6)$$

From (4), (5) and (6), we can express the instantaneous channel capacity for the primary link, the secondary data link and the secondary eavesdropping link respectively as given in (7)–(9)

$$C_{\text{PT,PR}}^{(m,u)} = \frac{1}{N_m + 1} \log_2 \left(1 + \psi_{\text{PT,PR}}^{(m,u)} \right), \quad (7)$$

$$C_{\text{T}_{m,u-1},\text{T}_{m,u}} = \frac{1}{N_m + 1} \log_2 \left(1 + \psi_{\text{T}_{m,u-1},\text{T}_{m,u}} \right), \quad (8)$$

$$C_{\text{T}_{m,u-1},\text{E}} = \frac{1}{N_m + 1} \log_2 \left(1 + \psi_{\text{T}_{m,u-1},\text{E}} \right), \quad (9)$$

where the factor $1/(1 + N_m)$ indicates that the data transmission of the secondary network is split into $(1 + N_m)$ orthogonal time slots.

To guarantee QoS of the primary network at any time slot, we focus on the lowest channel capacity of the $\text{PT} \rightarrow \text{PR}$ link, i.e.,

$$C_{\text{PT,PR}}^{m,\min} = \min_{u=1,2,\dots,N_m+1} \left(C_{\text{PT,PR}}^{(m,u)} \right). \quad (10)$$

Using (10), the outage probability (OP) of the primary network can be defined by

$$\text{OP}_m = \Pr \left(C_{\text{PT,PR}}^{m,\min} < R_P \right), \quad (11)$$

where R_P is a target rate of the primary network.

Considering the secondary network, the secrecy capacity at the u -th time slot is given as

$$\text{SC}_{m,u} = [C_{T_{m,u-1},T_{m,u}} - C_{T_{m,u-1},E}]^+, \quad (12)$$

where $[x]^+ = \max(0, x)$.

Due to the randomize-and-forward strategy, the end-to-end secrecy capacity obtained on the m -th path is expressed as

$$\text{SC}_m^{\text{e2e}} = \min_{u=1,2,\dots,N_m+1} (\text{SC}_{m,u}). \quad (13)$$

Then, the end-to-end PNSC on the m -th path is defined by

$$\text{PNSC}_m = \Pr(\text{SC}_m^{\text{e2e}} > 0). \quad (14)$$

3 Performance Evaluation

3.1 OP of Primary Network

In this sub-section, we calculate OP of the primary network when the m -th path is selected. Combining (7), (10) and (11), we can write

$$\text{OP}_m = 1 - \prod_{u=1}^{N_m+1} \left(1 - \Pr(\psi_{\text{PT,PR}}^{(m,u)} < \rho) \right), \quad (15)$$

where $\rho = 2^{((N_m+1)\text{R}_P)} - 1$. Substituting (4) into $\Pr(\psi_{\text{PT,PR}}^{(m,u)} < \rho)$ in (15), which yields

$$\begin{aligned} \Pr(\psi_{\text{PT,PR}}^{(m,u)} < \rho) &= \Pr\left(\gamma_{\text{PT,PR}} < \frac{P_{T_{m,u-1}}\rho}{P_{\text{PT}}}\gamma_{T_{m,u-1},\text{PR}} + \frac{P_{J_{m,u}}\rho}{P_{\text{PT}}}\gamma_{J_{m,u},\text{PR}} + \frac{\rho}{P_{\text{PT}}}\right) \\ &= \int_0^{+\infty} \int_0^{+\infty} \left[F_{\gamma_{\text{PT,PR}}} \left(\frac{P_{T_{m,u-1}}\rho}{P_{\text{PT}}}x + \frac{P_{J_{m,u}}\rho}{P_{\text{PT}}}y + \frac{\rho}{P_{\text{PT}}} \right) \right. \\ &\quad \left. - f_{\gamma_{T_{m,u-1},\text{PR}}}(x) f_{\gamma_{J_{m,u},\text{PR}}}(y) \right] dx dy. \end{aligned} \quad (16)$$

Substituting CDF and PDF given in (1) into (16), after some manipulation, we can obtain

$$\begin{aligned} \Pr(\psi_{\text{PT,PR}}^{(m,u)} < \rho) &= 1 - \frac{\lambda_{T_{m,u-1},\text{PR}} P_{\text{PT}}}{\lambda_{T_{m,u-1},\text{PR}} P_{\text{PT}} + \lambda_{\text{PT,PR}} P_{T_{m,u-1}}\rho} \\ &\quad \times \frac{\lambda_{J_{m,u},\text{PR}} P_{\text{PT}}}{\lambda_{J_{m,u},\text{PR}} P_{\text{PT}} + \lambda_{\text{PT,PR}} P_{J_{m,u}}\rho} \exp\left(-\frac{\lambda_{\text{PT,PR}}\rho}{P_{\text{PT}}}\right). \end{aligned} \quad (17)$$

Substituting (17) into (15), we obtain the exact closed-form expression for OP_m as follows:

$$\begin{aligned} \text{OP}_m &= 1 - \exp\left(-\frac{(N_m+1)\lambda_{\text{PT,PR}}\rho}{P_{\text{PT}}}\right) \\ &\quad \times \prod_{u=1}^{N_m+1} \left(\frac{\lambda_{T_{m,u-1},\text{PR}} P_{\text{PT}}}{\lambda_{T_{m,u-1},\text{PR}} P_{\text{PT}} + \lambda_{\text{PT,PR}} P_{T_{m,u-1}}\rho} \frac{\lambda_{J_{m,u},\text{PR}} P_{\text{PT}}}{\lambda_{J_{m,u},\text{PR}} P_{\text{PT}} + \lambda_{\text{PT,PR}} P_{J_{m,u}}\rho} \right). \end{aligned} \quad (18)$$

To guarantee the QoS of the primary network, the following condition should be satisfied:

$$\text{OP}_m \leq \varepsilon_{\text{OP}}, \quad (19)$$

where ε_{OP} is the target OP of the PT – PR link.

3.2 Power Allocation of Secondary Transmitters

This sub-section proposes a simple power allocation for the secondary transmitter to satisfy the required primary QoS. Firstly, we assume that all nodes in the cluster $\text{CL}_{m,u}$ have the same transmit power, i.e., $P_{\text{T}_{m,u}} = P_{\text{J}_{m,u}} = Q_{m,u}$ for all m, u . Secondly, if the distance between $\text{T}_{m,u}$ and PR is longer than that between $\text{T}_{m,v}$ and PR, $Q_{m,u}$ should be higher than $Q_{m,v}$, and vice versa, where $(u, v) \in \{0, 1, \dots, N_m + 1\}$ and $u \neq v$. Therefore, the ratio between $Q_{m,u}$ and $Q_{m,v}$ can be formulated as a function of the link distance as

$$\frac{Q_{m,u}}{Q_{m,v}} = \frac{d_{\text{T}_{m,u},\text{PR}}^\beta}{d_{\text{T}_{m,v},\text{PR}}^\beta} = \frac{\lambda_{\text{T}_{m,u},\text{PR}}}{\lambda_{\text{T}_{m,v},\text{PR}}} \Leftrightarrow \frac{Q_{m,u}}{\lambda_{\text{T}_{m,u},\text{PR}}} = \frac{Q_{m,v}}{\lambda_{\text{T}_{m,v},\text{PR}}} = \chi. \quad (20)$$

From (20), substituting $P_{\text{T}_{m,u}} = P_{\text{J}_{m,u}} = Q_{m,u} = \chi \lambda_{\text{T}_{m,u},\text{PR}}$ into (18), we arrive at

$$\text{OP}_m = 1 - \left(\frac{P_{\text{PT}}}{P_{\text{PT}} + \lambda_{\text{PT},\text{PR}} \chi \rho} \right)^{2(N_m+1)} \exp \left(- \frac{(N_m + 1) \lambda_{\text{PT},\text{PR}} \rho}{P_{\text{PT}}} \right). \quad (21)$$

Now, solving $\text{OP}_m = \varepsilon_{\text{OP}}$, we can express χ as

$$\chi = \frac{P_{\text{PT}}}{\lambda_{\text{PT},\text{PR}} \rho} \left[\left((1 - \varepsilon_{\text{OP}}) \exp \left(\frac{(N_m + 1) \lambda_{\text{PT},\text{PR}} \rho}{P_{\text{PT}}} \right) \right)^{-\frac{1}{2(N_m+1)}} - 1 \right]. \quad (22)$$

Because the transmit power $Q_{m,u}$ is not negative, we can provide an exact closed-form formula of $Q_{m,u}$ as follows:

$$Q_{m,u} = \frac{\lambda_{\text{T}_{m,u},\text{PR}} P_{\text{PT}}}{\lambda_{\text{PT},\text{PR}} \rho} \left[\left((1 - \varepsilon_{\text{OP}}) \exp \left(\frac{(N_m + 1) \lambda_{\text{PT},\text{PR}} \rho}{P_{\text{PT}}} \right) \right)^{-\frac{1}{2(N_m+1)}} - 1 \right]^+. \quad (23)$$

3.3 End-to-End PNSC of m -th Path

For the m -th path, the end-to-end PNSC can be formulated as

$$\begin{aligned} \text{PNSC}_m &= \prod_{u=1}^{N_m+1} \Pr \left(\frac{Q_{m,u-1} \gamma_{\text{T}_{m,u-1},\text{T}_{m,u}}}{P_{\text{PT}} \gamma_{\text{PT},\text{T}_{m,u}} + 1} > \frac{Q_{m,u-1} \gamma_{\text{T}_{m,u-1},\text{E}}}{P_{\text{PT}} \gamma_{\text{PT},\text{E}} + Q_{m,u} \gamma_{\text{J}_{m,u},\text{E}} + 1} \right) \\ &= \prod_{u=1}^{N_m+1} \Pr (Z_u^{\text{D}} > Z_u^{\text{E}}), \end{aligned} \quad (24)$$

where

$$Z_u^D = \frac{\gamma_{T_m, u-1, T_m, u}}{P_{PT}\gamma_{PT, T_m, u} + 1}, \quad Z_u^E = \frac{\gamma_{T_m, u-1, E}}{P_{PT}\gamma_{PT, E} + Q_{m, u}\gamma_{J_m, u, E} + 1}. \quad (25)$$

Furthermore, we can rewrite $\Pr(Z_u^D > Z_u^E)$ in (25) as

$$\Pr(Z_u^D > Z_u^E) = \int_0^{+\infty} (1 - F_{Z_u^D}(x)) f_{Z_u^E}(x) dx. \quad (26)$$

Next, we find the CDF $F_{Z_u^D}(x)$ which can be formulated by

$$F_{Z_u^D}(x) = \Pr(Z_u^D < x) = \int_0^{+\infty} F_{\gamma_{T_m, u-1, T_m, u}}(P_{PT}xy + x) f_{\gamma_{PT, T_m, u}}(y) dy. \quad (27)$$

Since $\gamma_{T_m, u-1, T_m, u} = \max_{v=1, 2, \dots, L_{m, u}} (\gamma_{T_m, u-1, R_{m, u, v}})$, we can obtain the CDF $F_{\gamma_{T_m, u-1, T_m, u}}(P_{PT}xy + x)$ as

$$\begin{aligned} F_{\gamma_{T_m, u-1, T_m, u}}(P_{PT}xy + x) &= (1 - \exp(-\lambda_{T_m, u-1, T_m, u}(P_{PT}xy + x)))^{L_{m, u}} \\ &= 1 + \sum_{v=1}^{L_{m, u}} (-)^v C_{L_{m, u}}^v \exp(-v\lambda_{T_m, u-1, T_m, u}x) \exp(-v\lambda_{T_m, u-1, T_m, u}P_{PT}xy). \end{aligned} \quad (28)$$

It is noted that when $u = N_m + 1$, then $L_{m, N_m+1} = 1$ and

$$\begin{aligned} F_{\gamma_{T_m, N_m, T_m, N_m+1}}(P_{PT}xy + x) &= \\ &= 1 - \exp(-\lambda_{T_m, N_m, T_m, N_m+1}x) \exp(-\lambda_{T_m, N_m, T_m, N_m+1}P_{PT}xy). \end{aligned} \quad (29)$$

Substituting (28) and $f_{\gamma_{PT, T_m, u}}(y) = \lambda_{PT, T_m, u} \exp(-\lambda_{PT, T_m, u}y)$ into (27), after algebraic simplifications, we obtain

$$\begin{aligned} F_{Z_u^D}(x) &= 1 + \sum_{v=1}^{L_{m, u}} \frac{(-)^v C_{L_{m, u}}^v \lambda_{PT, T_m, u}}{\lambda_{PT, T_m, u} + v\lambda_{T_m, u-1, T_m, u}P_{PT}x} \exp(-v\lambda_{T_m, u-1, T_m, u}x) \\ &= 1 + \sum_{v=1}^{L_{m, u}} (-)^v C_{L_{m, u}}^v \frac{\omega_{0, u, v}}{\omega_{0, u, v} + x} \exp(-v\lambda_{T_m, u-1, T_m, u}x), \end{aligned} \quad (30)$$

where

$$\omega_{0, u, v} = \frac{\lambda_{PT, T_m, u}}{v\lambda_{T_m, u-1, T_m, u}P_{PT}}. \quad (31)$$

Similarly, the CDF of Z_u^E can be obtained as

$$\begin{aligned} F_{Z_u^E}(x) &= \int_0^{+\infty} \left[F_{\gamma_{T_m, u-1, E}}(P_{PT}xy + Q_{m, u}xz + x) \right] dydz \\ &= 1 - \frac{\lambda_{PT, E}}{\lambda_{PT, E} + \lambda_{T_m, u-1, E}P_{PT}x} \frac{\lambda_{T_m, u, E}}{\lambda_{T_m, u, E} + \lambda_{T_m, u-1, E}Q_{m, u}x} \exp(-\lambda_{T_m, u-1, E}x) \\ &= 1 - \frac{\omega_{1, u}}{\omega_{1, u} + x} \frac{\omega_{2, u}}{\omega_{2, u} + x} \exp(-\lambda_{T_m, u-1, E}x), \end{aligned} \quad (32)$$

where $\lambda_{J_{m,u},E} = \lambda_{T_{m,u},E}$, $\omega_{1,u} = \frac{\lambda_{PT,E}}{\lambda_{T_{m,u-1},E}P_{PT}}$ and $\omega_{2,u} = \frac{\lambda_{T_{m,u},E}}{\lambda_{T_{m,u-1},E}Q_{m,u}}$.

Assume that $\omega_{1,u} \neq \omega_{2,u}$, the CDF $F_{Z_u^E}(x)$ can be rewritten as

$$F_{Z_u^E}(x) = 1 - \frac{\kappa_u}{\omega_{1,u} + x} \exp(-\lambda_{T_{m,u-1},E}x) + \frac{\kappa_u}{\omega_{2,u} + x} \exp(-\lambda_{T_{m,u-1},E}x), \quad (33)$$

where $\kappa_u = \frac{\omega_{1,u}\omega_{2,u}}{\omega_{2,u}-\omega_{1,u}}$. Then, the PDF $f_{Z_u^E}(x)$ is obtained as

$$f_{Z_u^E}(x) = \frac{\kappa_u}{(\omega_{1,u} + x)^2} \exp(-\lambda_{T_{m,u-1},E}x) + \frac{\kappa_u \lambda_{T_{m,u-1},E}}{\omega_{1,u} + x} \exp(-\lambda_{T_{m,u-1},E}x) - \frac{\kappa_u}{(\omega_{2,u} + x)^2} \exp(-\lambda_{T_{m,u-1},E}x) - \frac{\kappa_u \lambda_{T_{m,u-1},E}}{\omega_{2,u} + x} \exp(-\lambda_{T_{m,u-1},E}x). \quad (34)$$

Using (26), (30) and (34), we have

$$\Pr(Z_u^D > Z_u^E) = \sum_{v=1}^{L_{m,u}} (-)^{v+1} C_{L_{m,u}}^v \omega_{0,u,v} \kappa_u \times (I_{1,u,v} - I_{2,u,v} + I_{3,u,v} - I_{4,u,v}), \quad (35)$$

where $\xi_{u,v} = v\lambda_{T_{m,u-1},T_{m,u}} + \lambda_{T_{m,u-1},E}$, and

$$\begin{aligned} I_{1,u,v} &= \int_0^{+\infty} \frac{1}{(\omega_{0,u,v} + x)(\omega_{1,u} + x)^2} \exp(-\xi_{u,v}x) dx, \\ I_{2,u,v} &= \int_0^{+\infty} \frac{1}{(\omega_{0,u,v} + x)(\omega_{2,u} + x)^2} \exp(-\xi_{u,v}x) dx, \\ I_{3,u,v} &= \int_0^{+\infty} \frac{\lambda_{T_{m,u-1},E}}{(\omega_{0,u,v} + x)(\omega_{1,u} + x)} \exp(-\xi_{u,v}x) dx, \\ I_{4,u,v} &= \int_0^{+\infty} \frac{\lambda_{T_{m,u-1},E}}{(\omega_{0,u,v} + x)(\omega_{2,u} + x)} \exp(-\xi_{u,v}x) dx. \end{aligned} \quad (36)$$

Now, we can rewrite the integral $I_{1,u,v}$ as

$$\begin{aligned} I_{1,u,v} &= \frac{1}{(\omega_{0,u,v} - \omega_{1,u})^2} \int_0^{+\infty} \frac{1}{\omega_{0,u,v} + x} \exp(-\xi_{u,v}x) dx \\ &\quad - \frac{1}{(\omega_{0,u,v} - \omega_{1,u})^2} \int_0^{+\infty} \frac{1}{\omega_{1,u} + x} \exp(-\xi_{u,v}x) dx \\ &\quad + \frac{1}{\omega_{0,u,v} - \omega_{1,u}} \int_0^{+\infty} \frac{1}{(\omega_{1,u} + x)^2} \exp(-\xi_{u,v}x) dx, \end{aligned} \quad (37)$$

where $\omega_{0,u,v} \neq \omega_{1,u}$. After algebraic simplifications, we obtain

$$\begin{aligned}
 I_{1,u,v} &= \frac{1}{(\omega_{0,u,v} - \omega_{1,u})^2} \exp(\omega_{0,u,v} \xi_{u,v}) E_1(\omega_{0,u,v} \xi_{u,v}) \\
 &\quad - \frac{1}{(\omega_{0,u,v} - \omega_{1,u})^2} \exp(\omega_{1,u} \xi_{u,v}) E_1(\omega_{1,u} \xi_{u,v}) \\
 &\quad + \frac{1}{\omega_{0,u,v} - \omega_{1,u}} \left(\frac{1}{\omega_{1,u}} - \xi_{u,v} \exp(\omega_{1,u} \xi_{u,v}) E_1(\omega_{1,u} \xi_{u,v}) \right), \quad (38)
 \end{aligned}$$

where $E_1(\cdot)$ is exponential integral [23]. Similarly, we have

$$\begin{aligned}
 I_{2,u,v} &= \frac{1}{(\omega_{0,u,v} - \omega_{2,u})^2} \exp(\omega_{0,u,v} \xi_{u,v}) E_1(\omega_{0,u,v} \xi_{u,v}) \\
 &\quad - \frac{1}{(\omega_{0,u,v} - \omega_{2,u})^2} \exp(\omega_{2,u} \xi_{u,v}) E_1(\omega_{2,u} \xi_{u,v}) \\
 &\quad + \frac{1}{\omega_{0,u,v} - \omega_{2,u}} \left(\frac{1}{\omega_{2,u}} - \xi_{u,v} \exp(\omega_{2,u} \xi_{u,v}) E_1(\omega_{2,u} \xi_{u,v}) \right). \quad (39)
 \end{aligned}$$

Next, the integrals $I_{3,u,v}$ and $I_{4,u,v}$ can be calculated, respectively as

$$\begin{aligned}
 I_{3,u,v} &= \frac{\lambda_{\Gamma_{m,u-1},E}}{\omega_{1,u} - \omega_{0,u,v}} \\
 &\quad \times [\exp(\omega_{0,u,v} \xi_{u,v}) E_1(\omega_{0,u,v} \xi_{u,v}) - \exp(\omega_{1,u} \xi_{u,v}) E_1(\omega_{1,u} \xi_{u,v})], \quad (40)
 \end{aligned}$$

$$\begin{aligned}
 I_{4,u,v} &= \frac{\lambda_{\Gamma_{m,u-1},E}}{\omega_{2,u} - \omega_{0,u,v}} \\
 &\quad \times [\exp(\omega_{0,u,v} \xi_{u,v}) E_1(\omega_{0,u,v} \xi_{u,v}) - \exp(\omega_{2,u} \xi_{u,v}) E_1(\omega_{2,u} \xi_{u,v})]. \quad (41)
 \end{aligned}$$

Substituting (38)–(41) into (35), we obtain the exact closed-form expression for $\Pr(Z_u^D > Z_u^E)$, which is then substituted into (24) to obtain PNSC_m .

3.4 Path-Selection Methods

For the BEST method, the best path is selected by the following strategy:

$$\text{Path } a : \text{SC}_a^{\text{e2e}} = \max_{m=1,2,\dots,M} (\text{SC}_m^{\text{e2e}}). \quad (42)$$

From (42), the end-to-end PNSC of the BEST method is computed by

$$\begin{aligned}
 \text{PNSC}_{\text{BEST}} &= \Pr(\text{SC}_a^{\text{e2e}} > 0) = 1 - \prod_{m=1}^M (1 - \Pr(\text{SC}_m^{\text{e2e}} > 0)) \\
 &= 1 - \prod_{m=1}^M (1 - \text{PNSC}_m). \quad (43)
 \end{aligned}$$

Then, substituting the expression for derived in Subsect. 3.3 into (43), we obtain an exact closed-form expression for the end-to-end PNSC using the BEST method.

However, the implementation of the BEST method which requires the instantaneous channel state information (CSIs) of all of the links appears complex. In practice, the statistical CSIs, i.e., average channel gain, can be readily obtained. Therefore, we propose the MAXV method, where the path providing the maximum average end-to-end PNSC is selected for the data transmission. Mathematically, we thus can write

$$\text{PNSC}_{\text{MAXV}} = \max_{m=1,2,\dots,M} (\text{PNSC}_m). \quad (44)$$

Finally, if the instantaneous and statistical CSIs of the data and/or eavesdropping and/or interference links are unknown because of the complexity, delay time constraint or the random presence of the eavesdropper, the random path selection (RAND) will be an appropriate solution. In this method, the end-to-end PNSC is expressed by

$$\text{PNSC}_{\text{RAND}} = \frac{1}{M} \sum_{m=1}^M \text{PNSC}_m. \quad (45)$$

In (45), due to the random selection, the probability that the m -th path is selected for the data transmission equals to $1/M$ for all values of m .

4 Simulation Results

In this section, we perform Monte Carlo simulations to verify the proposed theoretical results obtained in Sect. 3. For illustration purposes only, in all of the simulations, the path loss exponent (β) is fixed by 3, the target rate of the primary network (R_P) is set at 0.25, and the required QoS of the primary network (ε_{OP}) is assumed to 0.05. We also assume that there are three available paths between the source and the destination ($M = 3$), the number of clusters are 2, 3, 4 ($N_1 = 2, N_2 = 3, N_3 = 4$), and the number of nodes in each cluster is set at 3 ($L_{m,u} = 3, \forall u, v$).

For the simulation environment, we consider a two-dimensional plane Oxy, in which the secondary source S and the secondary destination D are placed at (0,0) and (1,0), respectively. In addition, the cluster nodes $R_{m,u,v}$ have the same location at $(u/(N_m + 1), 0)$, and the position of the eavesdropper E is (x_E, y_E) , where $m = 1, 2, 3, u = 1, 2, \dots, N_m$. For the primary network, the primary transmitter (PT) and the primary receiver (PR) have been located at $(x_{\text{PT}}, y_{\text{PT}})$ and $(x_{\text{PR}}, y_{\text{PR}})$, respectively.

In Fig. 3, we present the transmit power of the secondary transmitters of the first path ($N_1 = 2$), including the source (S or $T_{1,0}$), the selected receivers and jammers ($T_{1,1}, T_{1,2}, T_{1,3}$), as a function of the transmit power of PT (P_{PT}). As

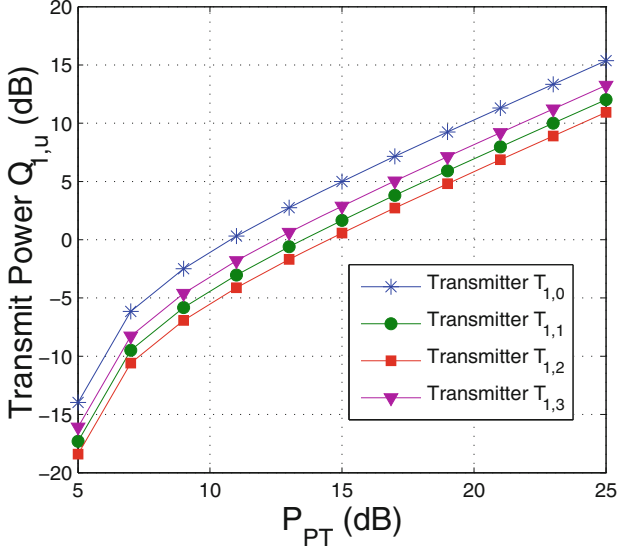


Fig. 3. Transmit power of the secondary transmitters on the first path as a function of P_{PT} in dB when $x_{PT} = 0.5$, $y_{PT} = 1$, $x_{PR} = 0.6$, and $y_{PR} = 0.6$.

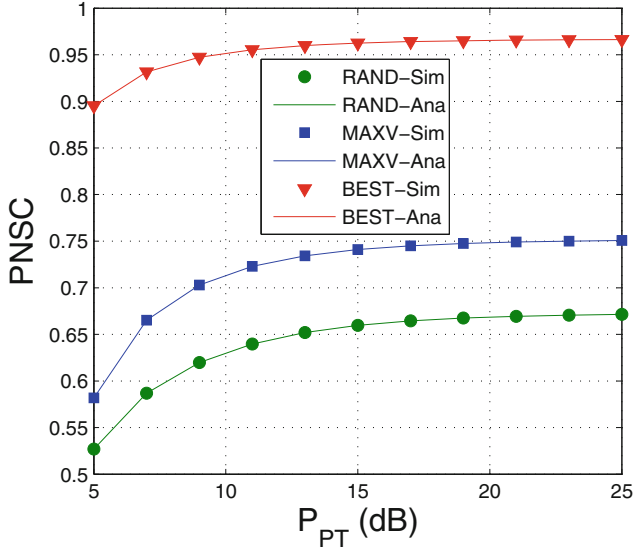


Fig. 4. End-to-end PNSC as a function of P_{PT} in dB when $x_{PT} = 0.5$, $y_{PT} = 1$, $x_{PR} = 0.5$, $y_{PR} = 0.75$, $x_E = 0.5$, and $y_E = -0.15$.

we can see, the transmit power $Q_{1,u}$ ($u = 0, 1, 2, 3$) increases as P_{PT} is increased. Indeed, as given in (23), $Q_{1,u}$ is an increasing function of (P_{PT}). Moreover, we can see in Fig. 3 that the transmit power of the source ($Q_{1,0}$) is highest because

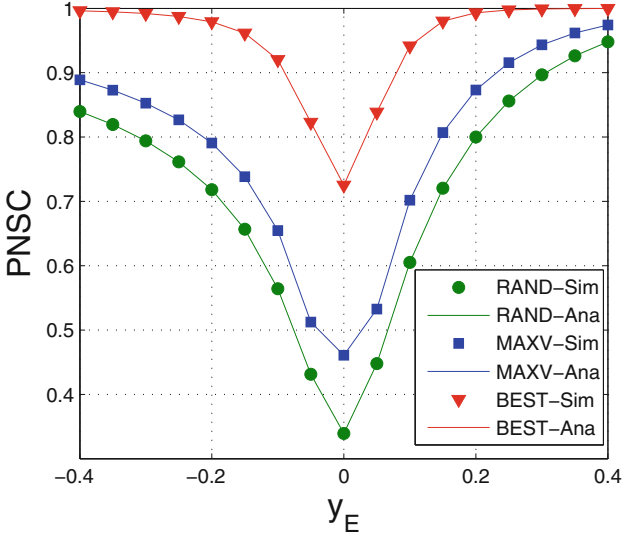


Fig. 5. End-to-end PNSC as a function of y_E when $P_{PT} = 15$ dB, $x_{PT} = 0.5$, $y_{PT} = 1$, $x_{PR} = 0.5$, $y_{PR} = 0.75$, $x_E = 0.5$, and $y_E = 0.5$.

the distance between the source and the primary receiver in this simulation is longest.

Figure 4 presents the end-to-end PNSC of the BEST, MAXV, RAND methods as a function of P_{PT} in dB. As shown, the BEST protocol obtains the highest performance, and the performance of the MAXV method is between that of the BEST and the RAND methods. It is shown that the PNSC performance of the proposed methods increases as P_{PT} is increased. However, as P_{PT} is high enough, the value of the end-to-end PNSC converges to a constant that does not depend on P_{PT} . Finally, we can observe that the simulation results (Sim) exactly match with the proposed theoretical results (Ana), which validates the correction of our derivations.

In Fig. 5, we study impact of the positions of the eavesdropper on the end-to-end PNSC. Particularly, we fix x_E by 0.5, and change y_E from -0.4 to 0.4 . It can be observed from Fig. 5 that the position of E significantly impacts the end-to-end PNSC. It is due to the fact that the eavesdropper is close to the transmitters, the PNSC performance is worse, and vice versa. As we can see in Fig. 5, when $y_E = 0$, the performance of the proposed methods is at its worst because the eavesdropper is at the nearest to the secondary transmitters. Again, consistent matching for the simulation and theoretical results has been achieved, which verifies our proposed theoretical analyzes.

5 Conclusion

In this paper, we have proposed and evaluated secrecy performance of three path-selection methods over cluster-based underlay CR networks by computing their end-to-end PNSC. Our results have shown that the BEST method attained the best performance, while that of the RAND method has appeared to be the worst. However, the implementation of the RAND and MAXV methods has been much simpler than the BEST method, which thus has presented trade-off between method complexity and secrecy performance. Moreover, the position of the eavesdropper and the transmit power of the primary transmitter significantly has impacted the end-to-end PNSC performance of the proposed methods. Future work on analyzing the proposed methods under more advanced fading environments will also be presented in a separate publication.

Acknowledgment. This research is funded by Vietnam National Foundation for Science and Technology Development (NAFOSTED) under grant number 102.04-2017.317.

References

1. Gopala, P.K., Lai, L., Gamal, H.E.: On the secrecy capacity of fading channels. *IEEE Trans. Inf. Theory* **54**(10), 4687–4698 (2008)
2. Zhang, J., Duong, T.Q., Woods, R., Marshall, A.: Securing wireless communications of the internet of things from the physical layer. *Overv. Entropy* **19**(8), 420 (2017)
3. Yang, N., Yeoh, P.L., Elkashlan, M., Schober, R., Collings, I.B.: Transmit antenna selection for security enhancement in MIMO wiretap channels. *IEEE Trans. Commun.* **61**(1), 144–154 (2013)
4. Xiong, J., Tang, Y., Ma, D., Xiao, P., Wong, K.-K.: Secrecy performance analysis for TAS-MRC system with imperfect feedback. *IEEE Trans. Inf. Forensics Secur.* **10**(8), 1617–1629 (2015)
5. Zhao, R., Lin, H., He, Y.-C., Chen, D.-H., Huang, Y., Yang, L.: Secrecy performance of transmit antenna selection for MIMO relay systems with outdated CSI. *IEEE Trans. Commun.* **66**(2), 546–559 (2018)
6. Krikidis, I.: Opportunistic relay selection for cooperative networks with secrecy constraints. *IET Commun.* **4**(15), 1787–1791 (2010)
7. Yang, M., Guo, D., Huang, Y., Duong, T.Q., Zhang, B.: Secure multiuser scheduling in downlink dual-hop regenerative relay networks over Nakagami-m fading channels. *IEEE Trans. Wirel. Commun.* **15**(12), 8009–8024 (2016)
8. Qing, L., Guangyao, H., Xiaomei, F.: Physical layer security in multi-hop AF relay network based on compressed sensing. *IEEE Commun. Lett.* **22**(9), 1882–1885 (2018)
9. Hoang, T.M., Duong, T.Q., Vo, N.-S., Kundu, C.: Physical layer security in cooperative energy harvesting networks with a friendly jammer. *IEEE Wirel. Commun. Lett.* **6**(2), 174–177 (2017)
10. Ma, H., Cheng, J., Wang, X., Ma, P.: Robust MISO beamforming with cooperative jamming for secure transmission from perspectives of QoS and secrecy rate. *IEEE Trans. Commun.* **66**(2), 767–780 (2018)

11. Duy, T.T., Kong, H.Y.: Secrecy performance analysis of multihop transmission protocols in cluster networks. *Wirel. Pers. Commun.* **82**(4), 2505–2518 (2015)
12. Tin, P.T., Duy, T.T., Phuong, T.T., Voznak, M.: Secrecy performance of joint relay and jammer selection methods in cluster networks: with and without hardware noises. In: *International Conference on Advanced Engineering - Theory and Applications*, Busan, pp. 769–779 (2016)
13. Lee, J.-H.: Full-duplex relay for enhancing physical layer security in multi-hop relaying systems. *IEEE Commun. Lett.* **19**(4), 525–528 (2015)
14. Atapattu, S., Ross, N., Jing, Y., He, Y., Evans, J.S.: Physical-layer security in full-duplex multi-hop multi-user wireless network with relay selection. *IEEE Trans. Wirel. Commun.* **18**(2), 1216–1232 (2019)
15. Liu, Y., Wang, L., Duy, T.T., Elkashlan, M., Duong, T.Q.: Relay selection for security enhancement in cognitive relay networks. *IEEE Wirel. Commun. Lett.* **4**(1), 46–49 (2015)
16. Nguyen, V.D., Duong, T.Q., Dobre, O.A., Shin, O.-S.: Joint information and jamming beamforming for secrecy rate maximization in cognitive radio networks. *IEEE Trans. Inf. Forensics Secur.* **11**(11), 2609–2623 (2016)
17. Liu, Y., Wang, L., Zaidi, S.A.R., Elkashlan, M., Duong, T.Q.: Secure D2D communication in large-scale cognitive cellular networks: a wireless power transfer model. *IEEE Trans. Commun.* **64**(1), 329–342 (2016)
18. Li, M., Yin, H., Huang, Y., Wang, Y., Yu, R.: Physical layer security in overlay cognitive radio networks with energy harvesting. *IEEE Trans. Veh. Technol.* **67**(11), 11274–11279 (2018)
19. Xu, Q., Ran, P., He, H., Xu, D.: Security-aware routing for artificial-noise-aided multi-hop secondary communications. In: *IEEE Wireless Communications and Networking Conference*, pp. 1–6. IEEE, Barcelona (2018)
20. Tin, P.T., Hung, D.T., Tan, N.N., Duy, T.T., Voznak, M.: Secrecy performance enhancement for underlay cognitive radio networks employing cooperative multi-hop transmission with and without presence of hardware impairments. *Entropy* **221**(2), 217 (2019)
21. Tin, P.T., Nam, P.M., Duy, T.T., Phuong, T.T., Voznak, M.: Secrecy performance enhancement for underlay cognitive radio networks employing cooperative multi-hop transmission with and without presence of hardware impairments. *Sensors* **19**(5), 1160 (2019)
22. Laneman, J.N., Tse, D.N., Wornell, G.W.: Cooperative diversity in wireless networks: efficient protocols and outage behavior. *IEEE Trans. Inf. Theory* **50**(12), 3062–3080 (2004)
23. Gradshteyn, I.S., Ryzhik, I.M.: *Table of Integrals, Series, and Products*, 7th edn. Elsevier Inc., San Diego (2007)